Materials Research Letters ›
Volume 4, 2016 - Issue 3

Open access

30,513 Views | 690 CrossRef citations to date | 0 Altmetric

Listen

Original Reports

Back stress strengthening and strain hardening in gradient structure

Muxin Yang, Yue Pan, Fuping Yuan, Yuntian Zhu & Xiaolei Wu

Pages 145-151 | Received 14 Jan 2016, Accepted 08 Feb 2016, Published online: 02 Mar 2016

Cite this article | https://doi.org/10.1080/21663831.2016.1153004 | Check for updates

Abstract

We report significant back stress strengthening and strain hardening in gradient structured (GS) interstitial free (IF) steel. Back stress is long-range stress caused by the pileup of [illegible] and a procedu[illegible]ysics from the tens[illegible]mechanical incompa[illegible]which needs to be ac[illegible]h but also signi[illegible]

Impact S[illegible]o increase strengthe[illegible] back stress fr[illegible]

GRAPH[illegible]

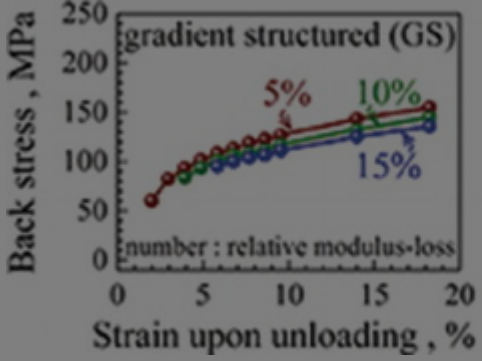

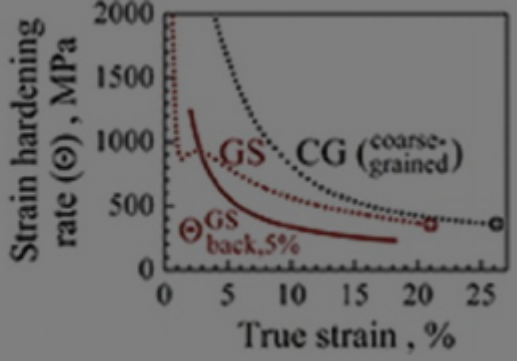

Keywords: Back Stress | Geometrically Necessary Dislocations | Work Hardening | Ductility | Gradient Structure

Gradient structure in metals represents a new strategy for producing a superior combination of high strength and good ductility.[1–6] The gradient structure usually consists of a nanostructured (NS) surface layer with increasing grain size along the depth to reach coarse-grained (CG) sizes in the central layer.[2,4]

Gradient structure can promote ductility significantly,[2,4–9] which is measured under tensile loading. The NS layer in a gradient structure may sustain a large amount of tensile strain,[2,4] because they are constrained by the CG layer. It was reported that the gradient structured (GS) Cu derives its ductility from the confinement of the soft CG core,[2,10] and from strong grain growth in the NS layer by mechanically driven grain growth during tensile deformation. Nanostructures in high-purity copper are known to be unstable at room temperature, and mechanical-driven grain growth in nanocry s with stable gradient hardening due to th h generates geometr and interacti s observed to pr h higher than] which is attribute tween layers.[3

The natu lear.[1,2] In fact, the on of many thin layers with increasing grain sizes.[3,4] The gradient structure deforms

heterogeneously due to plastic incompatibilities between neighboring layers with different flow behaviors and stresses under applied strains. As such, it is reasonable to anticipate the development of the strain gradient and internal stresses during plastic deformation, as a result of the plastic incompatibilities between different layers, similar to what happens in composites [19–21] and dual-phase structures.[22]

Back stress has been reported to play a crucial role in strain hardening, strengthening and mechanical properties.[21–23] It is a type of long-range stress exerted by GNDs that are accumulated and piled up against barriers. It interacts with mobile dislocations to affect their slip.[24] The back stress reduces the effective resolved shear stress for dislocation slip because it always acts in the opposite direction of the applied resolved shear stress. In a heterogeneous structure, strain will be inhomogeneous but continuous, producing strain gradients, which needs to be accommodated by GNDs.[23,25–27] It has been observed that back stress strengthening and back stress strain-hardening are primarily responsible for unprecedented combination of strength and ductility of heterogeneous lamella Ti, which was found as strong as ultrafine-grained Ti and as ductile as CG Ti.[23] The gradient structure can be regarded as a type of heterogeneous structure. Therefore, it is reasonable to assume that significant back stress will be developed in gradient structure, which should be investigated to have a better understanding on the fundamentals of gradient structure.

Here we report for the first time unambiguous experimental evidences of significant back stress hardening in GS IF steel. We will also derive an equation with sound physics to calculate back stress from an unloading–reloading stress–strain hysteresis loop during a m the hysteres

A 1-mm terials with the com P, 0.037% Al, 0.063% aled at 1173 grain size of 35 μm duce the GS sample. er of 120 μm thick num grain size of < ins with dislocati on was detailed in our previous papers.[3,4]

Unloading–reloading process during tensile tests was conducted using an Instron 5966 machine at a strain rate of $5 \times 10^{-4}\,s^{-1}$ at room temperature. Tensile specimens with a gauge length of 10 mm and a width of 2.5 mm were cut from SMAT-processed disks. An extensometer was used to measure tensile strain. At a certain unloading strain, the specimen was unloaded in a load-control mode to 20 N at an unloading rate of 200 N min^{-1}, followed by reloading to the same applied load.

Figure 1(a) shows the monotonic tensile true stress–true strain (σ–) curves in both GS and CG samples. The GS sample shows large tensile ductility comparable to that of CG, but with triple yield strength of CG, which is typical of the excellent combination of strength and ductility in GS metals.[2–8] A transient is visible soon after yielding, characterized by the presence of a short concave segment on the σ– curve.[4] During the transient, the strain hardening rate (Θ) sharply drops at first, which is followed by a rapid up-turn, as shown in Figure 1(b). Figure 1(c) shows the unloading and reloading test hysteresis loops measured at varying tensile strains for both CG and GS samples.

Figure 1. (Colour online) (a) Tensile stress–strain curves in the GS and CG IF steel samples. (b) Strain hardening rate ($\Theta = d\sigma/d$) vs. strain. (c) The unloading and reloading test hysteresis loops measured at varying tensile strains for both CG and GS samples.

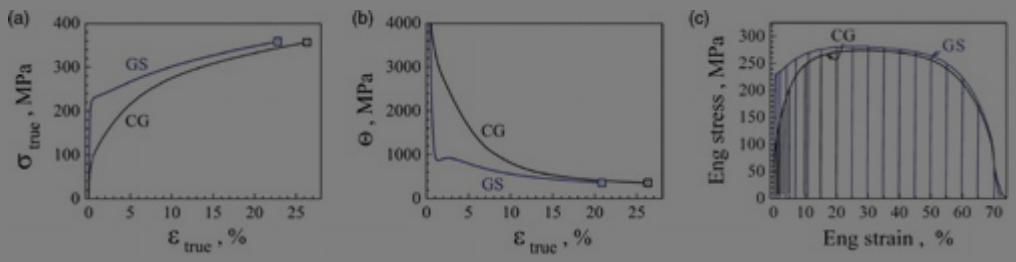

Unloadi the evolutio the unloadi starts at unloadi uasi-elastic and The stress drop i ,29] or viscous oading stress with an unloading yielding ing curve with EF an effective reloading Young's modulus of E_r, which can be assumed equal to E_u because the

microstructure is assumed not changed during the unloading–reloading. The point F is called the reloading yielding point, with a stress of σ_r. Figure 2(b) is the measured hysteresis loop from a GS IF steel sample.

Figure 2. (Colour online) (a) The schematic of the unloading–reloading loop for defining the unload yielding σ_u, reload yielding σ_r, back stress σ_b and frictional stress σ_f, effective unloading Young's modulus of E_u, effective reloading Young's modulus of E_r. (b) A measured hysteresis loop from the GS IF steel sample with σ_u and σ_r defined.

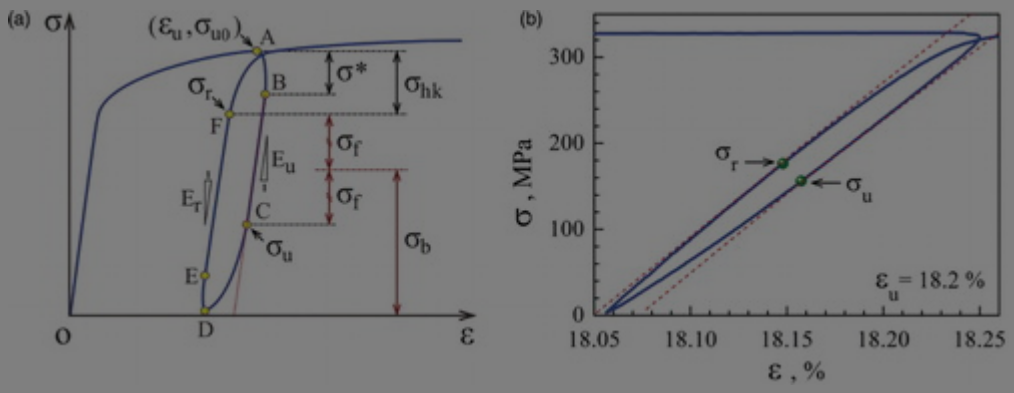

Display full size

From the unloading–reloading hysteresis loop, we can calculate the back stress σ_b, and the frictional stress σ_f. The back stress is always in the opposite direction of the applied stress, while frictional stress is always in the direction that opposes the motion of dislocations. The frictional stress consists of the Peierls stress as well as other stresses that are needed to overcome the dynamic pinning of dislocations such as solute atoms, second phase, forest dislocations, dislocation debris, dislocation jogs, etc.

To derive ve first assume –reloading process. ng before the unlo cause the reverse GNDs that produce the unlo assumption is impor ng, the back stress is g direction to produ applied stress is ess and the frictiona

(1)

where σ_u is the unloading yield stress as defined in Figure 2(a).

During the reloading, the applied stress needs to overcome the back stress and the frictional stress to drive the dislocation forward at the reloading yield point F, which can be described as

(2)

where σ_r is the reloading yield stress as defined in Figure 2(a).

Here again, we assume that the back stress during reloading is the same as the back stress during unloading. This is reasonable because during the unloading–reloading process, dislocation configuration can be considered reversible.[32] Solving Equations (1) and (2) yields

(3)

and

(4)

Equation (3) is similar to an earlier equation proposed for cyclic loading by Cottrell [33] and Kulmann-Wilsdorf and Laird,[32] except they used σ_{u0}, the initial flow stress at the beginning of the unloading, in place of the σ_r, that is

(5)

where σ_{u0} is the initial unloading stress as defined in Figure 2(a).

We argue that Equation (3) is physically sounder than Equation (5) because we are defining unloading yield and reloading yield using the same criterion, that is, the same deviation of effective Young's modulus as discussed later. It has been recognized that Equation (5) overestimates the back stress, and was later modified by Dickson et al. to include t

where σ* (a),[24,29] which is

Equati ng yield stres come negative we expect Equatior sure σ_u before th mportant advanta sistent back stress va hysically

problematic because they implicitly used different criteria to define the unloading yield and reloading yield, which is physically unjustifiable.

To extract useful data from the unloading–reloading hysteresis loop, one needs to first determine the unloading yield stress σ_u and reloading yield stress σ_r. However, the real hysteresis loop (e.g. Figure 2(b)) is not as well defined as in Figure 2(a), and the practical extraction of the data is not straightforward.[31] The first step is to determine the elastic segments BC as well as its slope (the effective Young's modulus). The unloading yield point C is usually determined by a plastic strain offset in the range of 5×10^{-6} to 10^{-3}, which have been used by different research groups.[24,31,34–37] These offset values are arbitrary and are not well justified. Here we propose to use the deviation of the stress–strain slope from the effective Young's modulus as a physically sound method to determine the yield point. In this study, we choose 5%, 10%, and 15% slope reduction from the effective Young's modulus, E_u. If the strain hardening in the plastically deforming volume is ignored, the slope reduction should be equal to the volume fraction that is plastically deforming. For example, a 10% reduction in E_u means 10% of the sample volume is plastically deforming. We also propose to use $E_r = E_u$, and the same slope reduction values for determining both the unloading yield point and reloading yield point.

Figure 3 compares the evolution of the unloading yield stress, reloading yield stress, and back stress of the CG and GS IF steel samples with increasing tensile strain at which the unloading was initiated. Several features can be seen from the figure. First, the unloading yield stress is affected more than the reloading yield stress by the slope reductio . Second, using a l higher reloadin choice of slope re atter in the calculate vantage of Equatio y reported Equa samples increase S sample than in t tress in the GS samp Figure 3(b) and 3(d) value is used, th are

negative and therefore cannot be measured in the unloading curve. This makes it advantageous to use a smaller slope reduction value in determining the back stress.

Figure 3. (Colour online) Evolution of (a) unloading yield stress σ_u and reloading yield stress σ_r and (b) back stress with increasing unloading strain $_u$ for CG IF steel, and the evolution of (c) unloading/reloading yield stresses and (d) back stress with increasing $_u$ for GS IF steel. $\sigma_{b,5\%}$ represents the back stress calculated using 5% slope reduction from the effective Young's modulus.

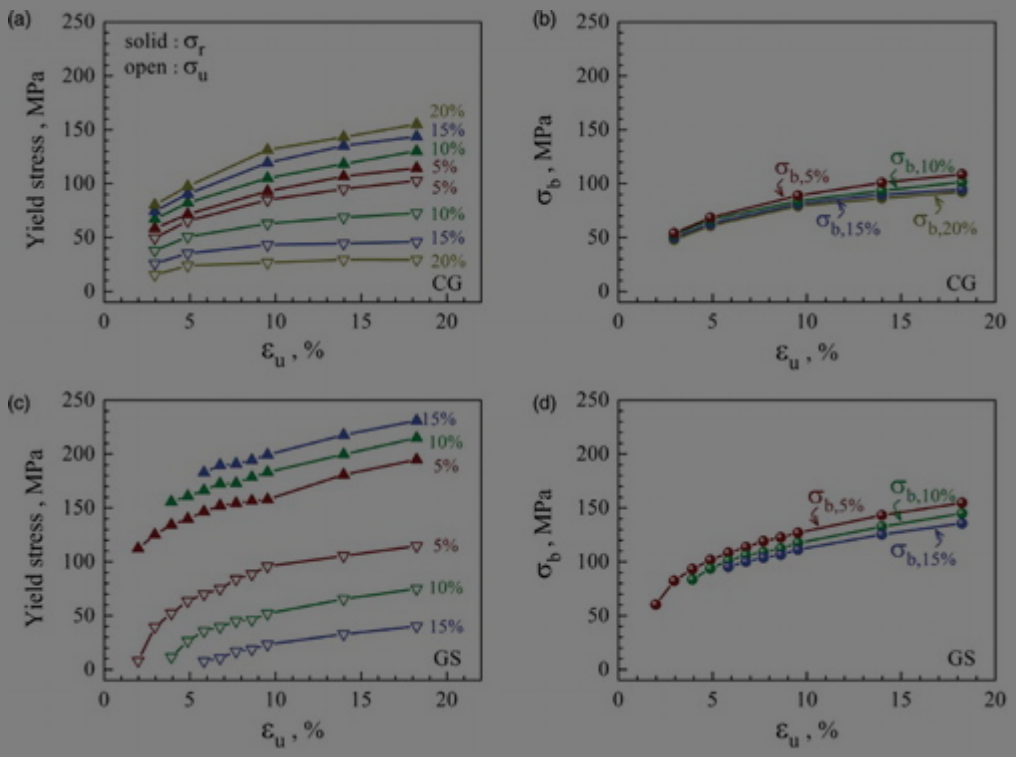

Display full size

For valid and easy comparison, we propose that the slope reduction value for calculati resents back stress ca lus, as shown ir g E_u, E_r, and the corre e linear parts of f these uncer

As show) is very scattere example, for the C es larger than tho on (4) adds the absc cancel each other as in Equation (3). Therefore, the frictional stress σ_f calculated using

Equation (4) is not quantitatively dependable. Nevertheless, Figure 4(a) consistently shows that for any slope reduction value, the calculated frictional stress is higher in the GS sample than in the CG sample. This is due to the higher dislocation density in the GS sample than in the CG sample.[3,4]

Figure 4. (Colour online) The frictional stress σ_f vs. tensile strain $_{true}$ for the GS and CG IF steel samples calculated according to Equation (4). (b) The distinct back stress hardening in GS IF steel. denotes the back stress hardening rate calculated using 5% slope reduction from the effective Young's modulus.

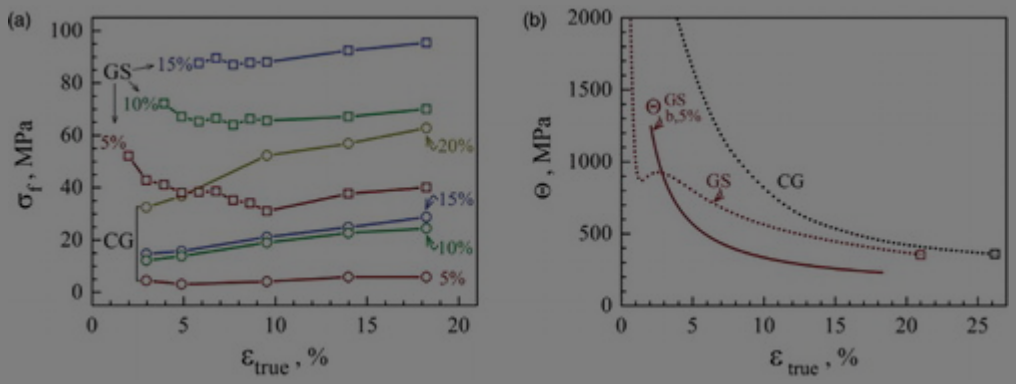

Display full size

Figure 4(b) shows that the GS sample has much higher back stress strain-hardening than the CG sample due to the heterogeneous microstructure, especially in the transient range that correlates to Θ up-turn. This indicates that the back stress strain-hardening has significant contribution to the observed Θ up-turn. The rapid back stress increase right after the yielding of the GS sample is also obvious in Figure 3(d). The observed Θ up-turn has been attributed to fast dislocation accumulation due to the back str ns.[4] The high bac gests that a large qu sociated with the here was a quick ind tion of the GS IF in which the N endicular to the tens ally, the surface stress, while the cent n is expecte

In summary, it is found that the GS IF steel developed strong back stress strengthening and back stress strain-hardening during tensile testing, which arise from the plastic incompatibilities due to its microstructural heterogeneity. The high back stress near the beginning of the plastic deformation of the GS IF steel samples should have contributed to the observed synergetic strengthening,[3] while the high back stress hardening should have contributed to the observed high ductility.[4] The equation derived and the procedure proposed in this work for calculating the back stress from the unloading–reloading hysteresis loop produces more consistent back stress value than what is previously reported.

Acknowledgements

This work was supported by the National Natural Science Foundation of China under Grant numbers (11572328, 11072243, 11222224, 11472286, and 51471039); and 973 Projects under Grant numbers (2012CB932203, 2012CB937500, and 6138504). Y.T.Z. is funded by the US Army Research Office (W911 NF-12–1–0009), the US National Science Foundation (DMT-1104667), and by the Jiangsu Key Laboratory of Advanced Micro&Nano Materials and Technology, Nanjing Univ of Sci and Technol.

Disclosure statement

No potential conflict of interest was reported by authors.

Refer

1. Lu
2014;

2. Fang T sticity in gradie

10.1126/science.1200177
PubMed | Web of Science ® | Google Scholar

3. Wu XL, JIang P, Chen L, et al. Synergetic strengthening by gradient structure. Mater Res Lett. 2014;2(4):185–191. doi: 10.1080/21663831.2014.935821
Web of Science ® | Google Scholar

4. Wu XL, Jiang P, Chen L, Yuan FP, Zhu YT. Extraordinary strain hardening by gradient structure. Proc Natl Acad Sci USA. 2014;111(20):7197–7201. doi: 10.1073/pnas.1324069111
PubMed | Web of Science ® | Google Scholar

5. Jerusalem A, Dickson W, Perez-Martin MJ, Dao M, Lu J, Galvez F, Grain size gradient length scale in ballistic properties optimization of functionally graded nanocrystalline steel plates. Scr Mater. 2013;69(11):773–776. doi: 10.1016/j.scriptamat.2013.08.025
Web of Science ® | Google Scholar

6. Wang HT, Tao NR, Lu K. Architectured surface layer with a gradient nanotwinned structure in a Fe-Mn austenitic steel. Scr Mater. 2013;68(1):22–27. doi: 10.1016/j.scriptamat.2012.05.041
Web of Science ® | Google Scholar

7. Kou HN, Lu J, Li Y. High-strength and high-ductility nanostructured and amorphous metall
10.10

8. Wei YJ ma in steel th 580.

9. Ma XL uctility in a coarse). doi: 10.10
Web of Science ® | Google Scholar

10. Fang TH, Tao NR, Lu K. Tension-induced softening and hardening in gradient nanograined surface layer in copper. Scr Mater. 2014;77:17–20. doi: 10.1016/j.scriptamat.2014.01.006
Web of Science ® | Google Scholar

11. Weertman JR. Retaining the nano in nanocrystalline alloys. Science. 2012;337(6097):921–922. doi: 10.1126/science.1226724
PubMed | Web of Science ® | Google Scholar

12. Chookajorn T, Murdoch HA, Schuh CA. Design of stable nanocrystalline alloys. Science. 2012;337(6097):951–954. doi: 10.1126/science.1224737
PubMed | Web of Science ® | Google Scholar

13. Zhang K, Weertman JR, Eastman JA. Rapid stress-driven grain coarsening in nanocrystalline Cu at ambient and cryogenic temperatures. Appl Phys Lett. 2005;87(6): Article no. 061921. doi: 10.1063/1.2008377
Web of Science ® | Google Scholar

14. Zhang K, Weertman JR, Eastman JA. The influence of time, temperature, and grain size on indentation creep in high-purity nanocrystalline and ultrafine grain copper. Appl Phys Lett. 2004;85:5197–5199. doi: 10.1063/1.1828213
Web of Science ® | Google Scholar

15. Legros
oundary
motio
14):3380–
3393.

16. Lia
JF, Zhu YT.
Hig
talline Ni.
Appl P

17. Li WB,
vith gradient
nano-grained structure. AIP Advances. 2015;5(8): Article no. 087120. doi:

10.1063/1.4928448
Google Scholar

18. Li JJ, Chen SH, Wu XL, Soh AK. A physical model revealing strong strain hardening in nano-grained metals induced by grain size gradient structure. Mater Sci Eng A. 2015;620:16–21. doi: 10.1016/j.msea.2014.09.117
Web of Science ® | Google Scholar

19. Llorca J, Needleman A, Suresh S. The Bauschinger effect in whisker-reinforced metal-matrix composites. Scr Metall Mater. 1990;24(7):1203–1208. doi: 10.1016/0956-716X(90)90328-E
Google Scholar

20. Sinclair CW, Saada G, Embury JD. Role of internal stresses in co-deformed two-phase materials. Philos Mag. 2006;86(25–26):4081–4098. doi: 10.1080/14786430600654438
Web of Science ® | Google Scholar

21. Thilly L, Van Petegem S, Renault PO, Lecouturier F, Vidal V, Schmitt B, Van Swygenhoven H. A new criterion for elasto-plastic transition in nanomaterials: application to size and composite effects on Cu-Nb nanocomposite wires. Acta Mater. 2009;57(11):3157–3169. doi: 10.1016/j.actamat.2009.03.021
Web of Science ® | Google Scholar

22. Calcag echanisms in fine- a ffect of aging.

23. Wu us lamella struct latl Acad Sci USA. 2

24. Feaugas X. On the origin of the tensile flow stress in the stainless steel AISI 316L at 300 K: back stress and effective stress. Acta Mater. 1999;47(13):3617–3632. doi: 10.1016/S1359-6454(99)00222-0
Web of Science ® | Google Scholar

25. Ashby MF. The deformation of plastically non-homogeneous materials. Philos Mag. 1970;21(170):399–424. doi: 10.1080/14786437008238426
Web of Science ® | Google Scholar

26. Gao H, Huang Y, Nix WD, Hutchinson JW. Mechanism-based strain gradient plasticity - I Theory. J Mech Phys Solids. 1999;47(6):1239–1263. doi: 10.1016/S0022-5096(98)00103-3
Web of Science ® | Google Scholar

27. Gao HJ, Huang YG. Geometrically necessary dislocation and size-dependent plasticity. Scr Mater. 2003;48(2):113–118. doi: 10.1016/S1359-6462(02)00329-9
Web of Science ® | Google Scholar

28. Lu K, Lu J. Nanostructured surface layer on metallic materials induced by surface mechanical attrition treatment. Mater Sci Eng A. 2004;375–377:38–45. doi: 10.1016/j.msea.2003.10.261
Web of Science ® | Google Scholar

29. Dicks measuring cyclic . doi: 10.10

30. Fo of the hys reep and stress ;437:197–211. d

31. Fournier B, Sauzay M, Caes C, Noblecourt M, Mottot M. Analysis of the hysteresis loops of a martensitic steel - Part I: study of the influence of strain amplitude and temperature under pure fatigue loadings using an enhanced stress partitioning method. Mater Sci Eng A. 2006;437:183–196. doi: 10.1016/j.msea.2006.08.086
Web of Science ® | Google Scholar

32. Kuhlmann-Wilsdorf D, Laird C. Dislocation behavior in fatigue II. Friction stress and back stress as inferred from an analysis of hysteresis loops. Mater Sci Eng. 1979;37(2):111–120. doi: 10.1016/0025-5416(79)90074-0
Google Scholar

33. Cottrell AH. Dislocations and plastic flow in crystals. Oxford: Clarendon Press; 1953.
Google Scholar

34. Delobelle P, Oytana C. The study of the laws of behavior at high-temperature, in plasticity-flow, of an austenitic stainless-steel (17–12-Sph). J Nucl Mater. 1986;139(3):204–227. doi: 10.1016/0022-3115(86)90174-1
Web of Science ® | Google Scholar

35. Risbet M, Feaugas X, Clavel M. Study of the cyclic softening of an under-aged gamma'-precipitated nickel-base superalloy (Waspaloy). Journal De Physique IV. 2001;11(PR4):293–301. doi: 10.1051/jp4:2001436
Google Scholar

36. Guille kinetics in nodula 2000;

37. Mo strain amplit 24–30. doi: 10.10

Related research

People also read | Recommended articles | Cited by 690